High power, room temperature, Terahertz sources and frequency comb based on Difference frequency generation at CQD.

Prof. Manijeh Razeghi [a)]

Center for Quantum Devices, Department of Electrical Engineering and Computer Science, Northwestern University, Evanston, Illinois 60208

ABSTRACT

Quantum cascade laser (QCL) is becoming the leading laser source in the mid-infrared and terahertz range due to its rapid development in power, efficiency, and spectral covering range. Owing to its unique intersubband transition and fast carrier lifetime, QCL possesses strong nonlinear susceptibilities that makes it the ideal platform for a variety of nonlinear optical generations. Among this, terahertz (THz) source based on difference-frequency generation (DFG) and frequency comb based on four wave mixing effect are the most exciting phenomena which could potentially revolutionize spectroscopy in mid-infrared (mid-IR) and THz spectral range. In this paper, we will briefly discuss the recent progress of our research. This includes high power high efficiency QCLs, high power room temperature THz sources based on DFG-QCL, room temperature THz frequency comb, and injection locking of high-power QCL frequency combs. The developed QCLs are great candidates as next generation mid-infrared source for spectroscopy and sensing.

Keywords: frequency comb, quantum cascade lasers, group velocity dispersion, four-wave mixing

1. INTRODUCTION

Quantum cascade laser (QCL) is a semiconductor laser based on intersubband transitions [1]. After near three decades of development, it has become the most important coherent light source in mid-infrared (mid-IR) and terahertz (THz) ranges. Many other application technologies, like spectroscopies capable of molecular absorption fingerprint measurement, medical imaging capable of in-depth observation and analysis of diseased tissues and organs, and free-space communications targeting faster, longer distance communications are benefiting from the rapid advancement of QCL technologies [2].

High performance in power, efficiency and spectral range are of fundamentally importance to the above QCL applications. Center for Quantum Device (CQD) in Northwestern University has been focused on QCL technology research and development in the past years [3-6]. Constant improvement in the structure design, material quality, and fabrication technologies, as well as the nonlinear effects for THz and frequency comb has been achieved. Previously, we has demonstrated high power room temperature continuous wave (CW) operation across a wide range of wavelength from 3.0 μm [7] to 145.6 μm [8], and the most powerful QCLs in room temperature CW operation with the highest WPE of 21% at 4.9 μm[9] and the highest power of 8.2 W at 8.1 μm [10]. In this paper, we present some

[a)] email: razeghi@northwestern.edu

of our recent breakthroughs in QCLs, discussed in detail in the following sections, on high power and high efficiency CW QCLs, high power room temperature THz sources based on DFG-QCL, room temperature THz frequency comb, and injection locking of high-power QCLs. The demonstrated QCLs are holding great promises for next generation mid-infrared spectroscopy and sensing.

2. HIGH POWER EFFICIENCY QUANTUM CASCADE LASER

The wall-plug efficiency (WPE) of a QCL represents the energy conversion efficiency from electrical power input to optical power output. Optimizing the WPE can not only efficiently take advantage of electrical energy, but also can minimize the waste heat produced within a laser, which can significantly improve the reliability of lasers, especially for QCLs under continuous-wave (CW) operation. Unlike traditional semiconductor lasers whose WPE is capable of exceeding ...70% at room temperature [11], it has proven to be challenging to improve the WPE of a QCL since a minimum voltage (typically above 10 V) is required to align the cascade structures before any gain behavior. Besides, lower quantum efficiency and stronger carrier thermalization during electron transport in minibands also prevent the increase of QCL WPE. In 2011, we reported a high performance QCL with ...21% WPE in CW operation and ...27% WPE in pulsed operation was demonstrated at room temperature [9]. This laser, based on the shallowwell design [12], consists of 40 QCL-stages and is featured by a high characteristic temperature T0 ≈ 240 K. Since then, no improvement of the CW WPE of QCLs has been reported. Although a newly designed QCL with ...28% pulsed WPE was demonstrated a few years ago, its CW performance is far below 21% due to a significantly lower characteristic temperature of T0 ≈ 140 K [13].

In fact, aside from further optimizing the quantum design of a QCL, its WPE can be also improved by increasing the thickness of the laser core (proportional to the number of QCL stages, N_s) as it can raise the waveguide optical confinement factor (Γ), reduce the waveguide loss (α_w), and lower the threshold current density (J_{th}). Lower waveguide loss permits increasing the WPE (η_{wpe}) by lifting the optical efficiency (η_o) since

$$\eta_{wpe} = \eta_o \cdot \eta_i \cdot \eta_v \cdot \eta_e \quad (1)$$

Here $\eta_o = \alpha_m/(\alpha_m+\alpha_w)$, where η_i, η_v, η_e, α_m is the internal quantum efficiency, voltage efficiency, electrical efficiency and mirror loss, respectively [4]. A higher confinement factor enables WPE improvement by decreasing the threshold current density, because less gain (g) is required to for lasing ($g = (\alpha_m+\alpha_w)/\Gamma$). However, increasing N_s will also increase the temperature of the laser core in CW operation, which will strongly degrade the performance. Thus, to achieve higher CW WPE, an optimization between the thickness increase and thermal accumulation is required.

On the other hand, the buried ridge regrowth process has been widely used in the fabrication of high-power cw QCLs. [4] After the formation of a laser ridge waveguide by wet etching two channels (...10 μm deep) on either side, the regrowth of semi-insulating Fe:InP cladding is performed by metalorganic chemical vapor deposition (MOCVD) to fill the channels. This will significantly reduce the optical loss and increase the thermal conductivity. Ideally, a complete planarization of the channels is desired to suppress any losses due to the processing. However, the planarization is difficult to achieve since the regrowth rate depends on many factors, including the opening width, volume of the channels, and density of the channel patterns. Overgrowth of Fe:InP is generally undesired because it would introduce thermal dissipation issues to devices bonded epilayer-down to a heat sink. Therefore, for past efforts, the channels were undergrown with 1–3 μm depth unfilled. This type of undergrowth for the devices can introduce air gaps in the channels during epi-layer down bonding, which will result in less effective heat dissipation for cw operation. Here, we redesign the buried ridge regrowth process and introduce a post-polishing technique, as the schematic shown in Fig. 1(a). Instead of undergrowth, the etched channels are intentionally overgrown by 3–5 μm to completely fill the empty channel. The 1-μm thick SiO_2 layer, which has been used as the hard mask for the regrowth, will be used as the protecting layer during the post-polishing treatment. This polishing step will not only flatten the overgrown channels but also remove any defects on top of the mask generated during the Fe:InP regrowth, which might later turn into failure spots after packaging. As the current increases, this temperature discrepancy will increase

as well. As a result, the planarized device exhibits improved reliability and performance compared with the undergrown devices.

Here, we report a post-polishing technique to achieve nearly complete surface planarization for the buried ridge regrowth processing of quantum cascade lasers [14]. The planarized device geometry improves the thermal conduction and reliability and, most importantly, enhances the power and efficiency in continuous wave operation. With this technique, we demonstrate a high continuous wave wall-plug efficiency of an InP-based quantum cascade laser reaching ...41% with an output power of ...12 W from a single facet operating at liquid nitrogen temperature. At room temperature, the continuous wave output power exceeds the previous record, reaching ...5.6 W.

Based on the above optimized processing, we take the design with the current state-of-the-art performance as a Ref. [9]. By increasing the QCL-stages from 40 to 45 and improving the quality of processing, as shown in Figures 1(b-c), we demonstrate a QCL, emitting at ...4.9 μm, which demonstrates the highest room temperature, pulsed WPE to date (29.3%). This design is also shown to be capable of delivering 5.6 W optical power in CW operation from a

single facet with an unprecedented WPE of 22% [15], as shown in Figure 1(e). An extremely high optical power density of ...35 MW/cm^2 has been achieved at room temperature without damaging the outcoupling facet. This result achieves an important milestone in CW QCL efficiency and output power and demonstrates the reproducibility of material growth and device fabrication quality. Then, we further increase the cascade stage number to 50, and demonstrate a quantum cascade laser emitting at $\lambda \approx 4.9$ μm with a wall-plug efficiency of ...31% and an output power of ...23 W in pulsed operation at room temperature [16], as shown in Figure 1(d).

The above performance optimization of mid-IR QCLs in power and efficiency would also benefit the various nonlinear effect studies.

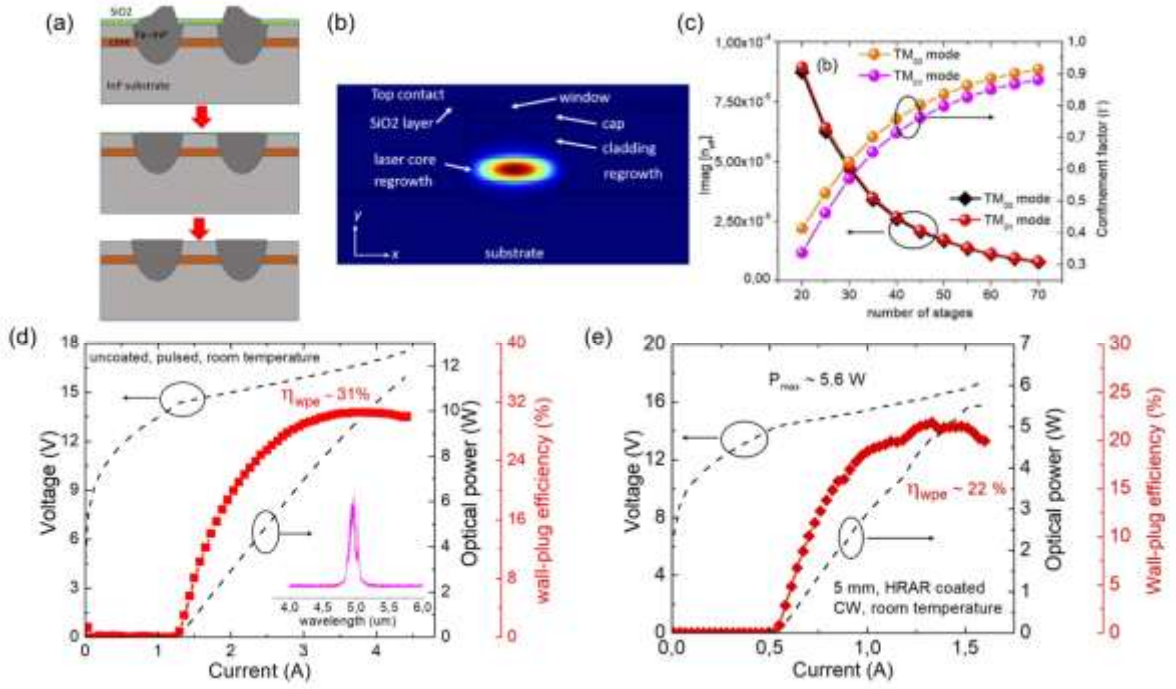

Fig. 1 (a) Schematic of planarized buried ridge process for high performance QCLs. (b) optical mode of a typical buried ridge waveguide

QCL. (c) Modal loss and confinement factor of QCL as functions of active region stage numbers. (d) P-I-V and WPE vs current curve of a QCL with active region stage number of 50, bonded epi-down under pulsed mode operation at room temperature. The inset of (c) shows the emission spectrum at 5.0μm. (e) P-I-V and WPE vs current curve of a QCL with active region stage number of 45, bonded epi-down under CW mode operation at room temperature.

3. HIGH POWER ROOM TEMPERATURE TERAHERTZ SOURCES AND FREQUENCY COMBS

The THz spectral range (1-10 THz) is extremely interesting for applications such as explosive and drug detection, security screening (T-ray imaging), astronomy, and medical imaging. One promising platform for THz technology is InP-based intracavity difference frequency generation using mid-IR quantum cascade lasers (QCLs), as shown in Fig. 2(a-b) [6,17]. This technique combines a dual frequency pump laser with engineered intersubband nonlinear susceptibility ($\chi^{(2)}$) to generate narrow linewidth THz radiation inside a single waveguide.

Thus, this type of THz source is free from the temperature limitation suffered by the THz QCLs based on direct optical transition, and ideally its working temperature is only limited by the mid-IR QCL which can work well even above 100 °C , and can be tuned over a broad waveguide range with broadband heterogeneous active region design [40]. It not only shares the common features of the mid-IR QCLs which are mass reproducible, room temperature operation, low cost, compact size, and high efficiency, but also carries the potential of delivering THz emission with high power in a wide frequency range.[18]

Besides providing a wealth of beautiful physics to study, this technique allows for compact, room temperature operation over a wide spectral range. Our group, utilizing state-of-the-art QCL technology, is making steady progress in this field in the following four aspects: stable THz frequency emission (Fig. 2(c)); high THz power with narrow emitting beam (Fig. 2(d)); continuous wave operation up to 14 μW and wide frequency tenability from 1-4.6 THz in pulsed mode operation (Fig. 2(e)) and 2.06-4.35 THz in continuous wave operation (Fig. 2(f)) [8, 19-23].

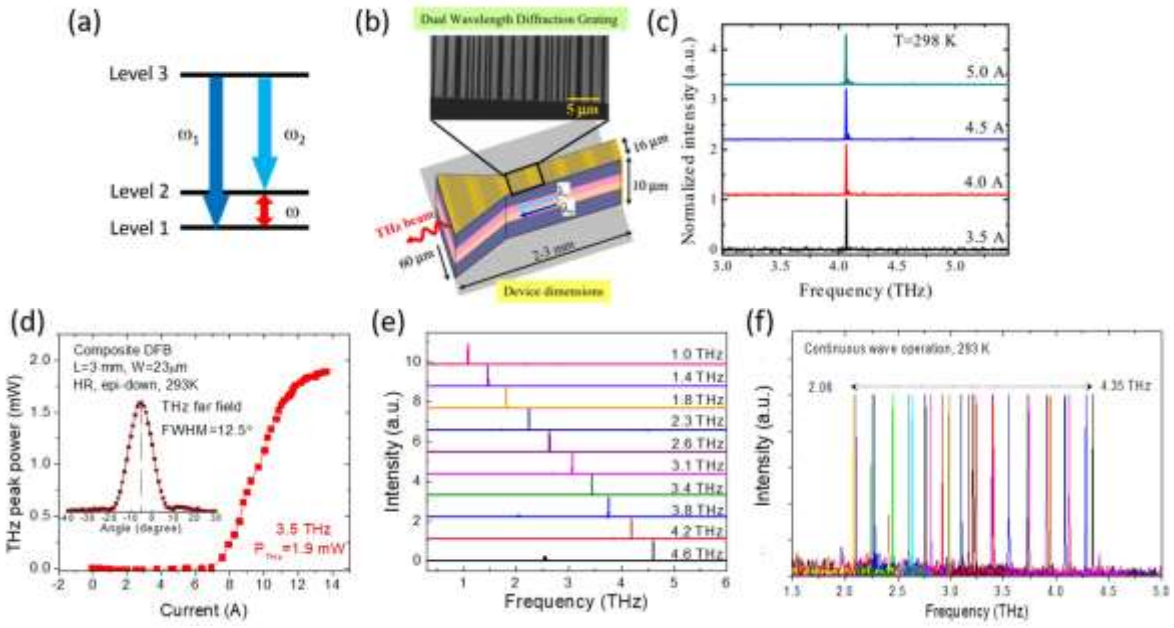

Fig. 2(a) Schematic of difference-frequency generation in mid-IR QCL. (b) Schematic composited DFB grating for dual-mode midIR operation and single mode THz emission. (c) Stable THz emitting spectra at different currents at room temperature. (d) Measured THz power of a THz source based on difference-frequency generation in mid-IR QCL at room temperature and its far field at 11 A in Inset. (e) THz step tuning from an array of THz QCL sources in pulsed mode operation. (f) Continuous wave THz tuning from two QCL sources in room temperature CW operation.

Frequency combs, spectra of phase-coherent equidistant lines, have revolutionized time and frequency metrology [24]. The recently developed quantum cascade laser (QCL) comb has exhibits great potential with high power and broadband spectrum [25-28]. However, in the terahertz (THz) range, cryogenic cooling has to be applied for THz QCL combs. Recently, we overcame this issue and reported a room temperature THz frequency comb at 3.0 THz based on difference-frequency generation from a mid-IR QCL comb [29]. A largely detuned distributedfeedback grating is integrated into the QCL cavity to provide the single mode operation as well as enhanced spatial hole-burning effect for multimode comb operation, as shown in Figure 3(a). Here, a largely detuned DFB grating is used to realize single mode and comb operation in the same cavity. The DFB wavelength position is detuned by ~8090 cm^{-1} with respect to the comb emission wavelength. Meanwhile, the grating coupling strength (κL , L= grating length) is set to be 3-5 to secure the single mode operation for the largely detuned DFB design. In the comb operating spectral range of 1240-1280 cm^{-1}, the calculated DFB dispersion is limited to ±1500 fs^2. The dispersion testing result reveals that limited dispersions are induced for the designed DFB device near the gain peak, which indicates the grating design will not pose a negative effect on the four-wave mixing for comb operation.

The DFB device emits a single mode at λ_1=7.25 μm defined by the grating period and a pronounced multimode emission at λ_2=7.81 μm simultaneously, as shown in Fig. 3(b). Instead of emitting dense-state fundamental comb as the FP device, the detuned DFB device produces stable multimode emissions with a mode spacing corresponding to 14 times the free spectral range (FSR) of the laser cavity for currents I≤1.5 A and 22 times the FSR at higher currents. Thanks to the mid-IR harmonic state comb operation with a limited mode number, the converted THz light intensity is concentrated on a limited number of comb modes with a side mode suppression ratio up to 20 dB (Fig. 3(e)). The THz power was measured with a calibrated Golay cell detector. The DC injecting current is modulated with a low frequency modulation to match the testing condition of the detector. The DFB device emits a continuous THz power up to 5 μW. Multiheterodyne spectroscopy with multiple equally spaced lines by beating it with a reference FabryPérot comb confirms the THz comb operation (Figs. 3(c-d)). This type of THz comb provides a new solution to chipbased high-speed high-resolution THz spectroscopy with compact size at room temperature.

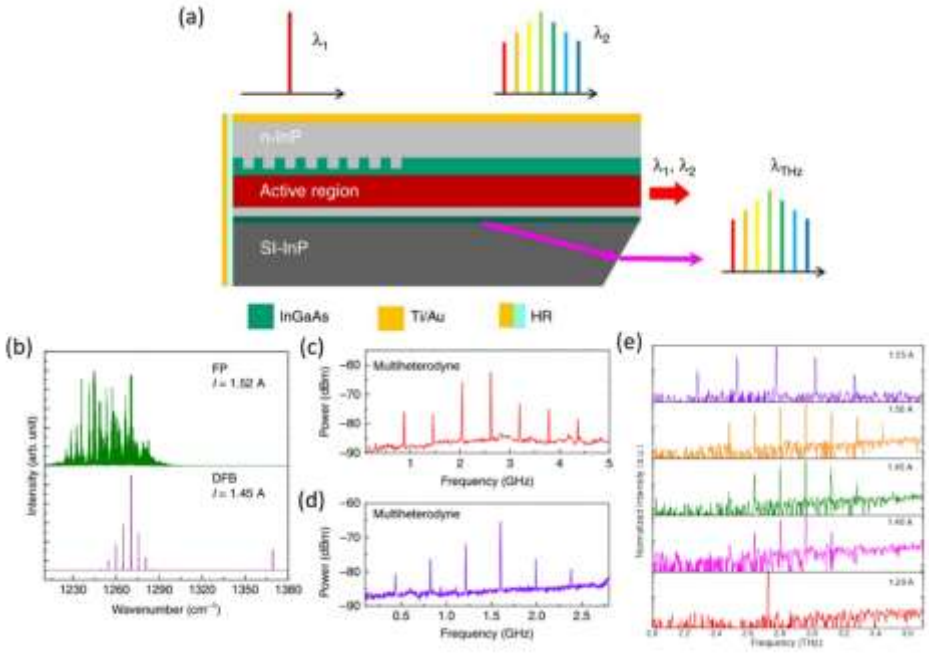

Fig. 3(a) Schematic of largely detuned DFB design for THz frequency comb based on QCL. (b) Multi-heterodyne characterizations based on the DFB and FP QCL combs. a Lasing spectrum of the FP comb at 1.52 A and the DFB comb at 1.45 A recorded with the FTIR, respectively. Multi-heterodyne beating of the FP comb at 1.52 A and the DFB comb at 1.45 A

(c), and the DFB comb at 1.55 A (d). (e) Lasing THz spectra of the DFB QCL comb evolving at different currents from 1.20 to 1.55 A at room temperature continuous wave operation.

4. INJECTION LOCKING OF HIGH-POWER QCLS

Injection locking was originally used to build a powerful and spectrally pure laser in the Master Oscillator Power Amplifier (MOPA) architecture, where a well-controlled low-power frequency stable laser is injected into a powerful but spectrally broad laser [30]. Then the spectral purity of the master laser can be transferred to the powerful slave laser. This technique shows great advantages for the amplification and stabilization of a single mode laser. However, for a multi-mode laser it is challenging, as it requires locking a few or even hundreds of longitudinal modes individually. Electrical injection locking is, therefore, developed to achieve the same goal through locking the inter-mode spacing, instead of longitudinal modes directly, of a semiconductor laser by applying a microwave signal that is resonant with its round-trip frequency. This approach has enabled active and hybrid modelocking of interband semiconductor lasers [31].

Harmonic injection locking is routinely used in the visible and near-infrared range to generate multiple light pulses within the photon round-trip time of a laser cavity. This provides the possibility to get high-repetition rate laser systems, which is of particular interest in high-bit rate optical communication [32], photonic analogue-to-digital conversion [33], multi-photon imaging [34], and astronomical frequency comb generation [35]. Owing to the intersub-band transition [3,4], the unique ultrafast gain recovery time of a quantum cascade laser (QCL) with picosecond

relaxation dynamics that is not present in other laser system is expected to overcome the limit of response to direct high-speed gain/loss modulation in classical semiconductor lasers. Therefore, harmonic, especially high order harmonic injection locking is inherently adapted to QCLs [36], which can potentially open up the prospect of applications of high-power, high-speed semiconductor lasers in the midinfrared range for frequency comb engineering, metrology, and the next-generation ultrahigh-speed telecommunication. This is in strong contrast to the traditional opinions that have considered these ultrafast dynamics of QCLs as an inhibitor and a bottleneck to the widespread use of these unipolar semiconductor lasers. Besides, high-order harmonic injection locking with modulation speed faster or equivalent to the gain recovery time of QCL might also provide the potential to generate ultrafast mid-infrared light pulses with extremely high repetition rate far beyond the current state of the art in semiconductor lasers. This has been one of the main challenges in the QCL community for many years despite some recently reported results [37,38].

Although injection locking of mid-infrared QCLs has been demonstrated, it was only applied to very low output power (<200 mW) and very low operating temperature (<80 K) devices [39,40], which strongly limits its broadranging applications across the domains of fundamental physics, high precision metrology, and wireless communication. Harmonic injection-locked QCLs have also been demonstrated recently in the terahertz (THz) range, but their output power is extremely low (...10 μW), even at liquid helium temperature (10 K) [36]. To date, no demonstration of harmonic injection locking of QCL has been done in the mid-infrared regime. In this work [39], we demonstrate for the first time to our knowledge the injection locking and harmonic injection locking of a midinfrared QCL at $\lambda \approx 8.2$ μm with an output power over 1 W in continuous-wave (CW) operation at 288 K. We also examined the experimental results in the theoretical framework of injection locking. They are well in agreement with each other. Varying the operating temperature of the injection-locked QCL within 1°C, its intermode spacing fluctuation can be still stabilized to hertz level by the external microwave modulation up to ...18 GHz.

The experimental setup is schematically illustrated in Fig. 4. The high-performance QCL is biased at 1165 mA using a low-noise current source (Wavelength Electronics QCL2000). The QCL emission is coupled into a quantum well infrared photodetector (QWIP) for beat note measurements. The tunable RF signal is first amplified and then injected into the QCL through a high-speed, low-loss RF waveguide. This coplanar waveguide, capable of

transmitting signals from DC up to >100 GHz, significantly lowers the connection losses and permits efficient RF power injection for high-power QCL locking.

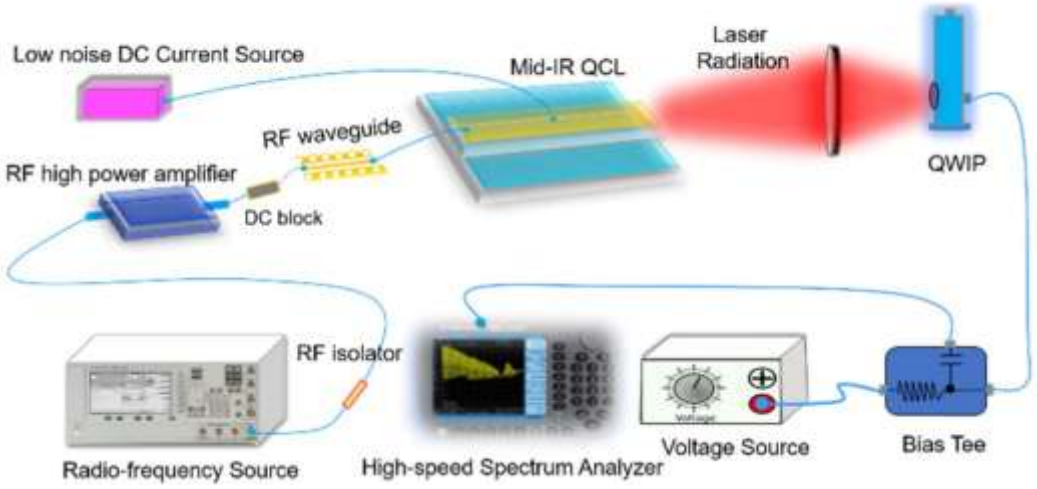

Fig. 4(a) Experimental setup. The mid-infrared QCL is biased by a low-noise DC current source. Laser emission is coupled into a quantum well infrared photodetector (QWIP). The high frequency components of the photocurrents are coupled into a spectrum analyzer. RF waves are generated by a RF generator and amplified by a high-power amplifier. The RF signal is injected into the QCL through a high-speed RF waveguide from near the back facet of the QCL.

Prior to investigating harmonic injection locking, we firstly demonstrate the fundamental injection locking of a midinfrared QCL with watt-level output power in CW operation at high temperature (288 K). In a QCL system, the electrical beating of the quasi-equally spaced Fabry–Perot modes (f_n) will generate a beat note signal that can be expressed as $S(f) = \sum S(f + f)$. The bandwidth of the beat note depends on the fluctuation of the intermode spacings of the laser. As shown in Figs. 5(a) and 5(b), the beat note of the QCL used in this paper is located at f beatnote ≈ 8964 MHz when the laser is biased at 1164 mA. Similar to optical injection locking, by injecting an RF signal (f_{RF}) that is resonant with the beat note frequency ($f_{beatnote}$) into the QCL system, the spectral purity and stability of the low-noise external RF signal can be transferred to the beat note through light–matter interaction. From the complex amplitude evolution of the RF field in the system, the injection locking can be described using the following equation:

$$\frac{d\varphi}{dt} = \omega_{RF} - \Delta\omega - \omega_L \sin\varphi. \tag{2}$$

Here φ is the phase difference between the injected RF signal and the beat note signal, ω_{RF} is the angular frequency of the RF signal, Δω is the angular frequency of the beat note, and $\omega_L \sim (P_{inj}/P_0)^{1/2}$ is the locking range, determined by the injected RF power P_{inj} and the intracavity laser power P_0. When $|\omega_{RF} - \Delta\omega| < \omega_L$, Eq. (2) has steady-state solution: $\sin\varphi = (\omega_{RF} - \Delta\omega)/\omega_L$. In this case, the beat note is resonant with the injected RF signal. When $|\omega_{RF} - \Delta\omega| > \omega_L$, Eq. (2) can no longer have any steady-state solution, falling out of the locking range.

With an injection current of 1165 mA, the output power of the QCL is over 1 W in CW operation at 288 K as shown in Fig. 1(b). At this operating condition, we inject an RF frequency into the QCL system and increase it step by step from 8963.560 to 8965.395 MHz. Intuitively, the beat note evolution process can be divided into three regimes as shown in Fig. 5(a). (i) Within [8963.560 MHz, 8964.395 MHz], the beat note is pulled toward the RF frequency from 8964.615 to 8964.395 MHz. This is out of injection locking. (ii) From 8964.395 to 8964.740 MHz, the beat note is in resonance with the RF signal, and their frequencies are clamped to each other ($f_{beatnote} = f_{RF}$). (iii) From 8964.740 to 8965.395 MHz, the laser goes beyond the resonance regime again, and the beat note gradually moves away from

the RF signal. When the RF signal is off-resonance with the laser system, the linewidth (FWHM) of the beat note is on the order of 90 kHz. While they are in resonance, the beat note linewidth dramatically drops down to hertz level (20 Hz) as shown in Fig. 3(b). This phenomenon revealed that the mid-infrared QCL is greatly stabilized, and its intermode spacing fluctuation is decreased by a factor above 1×10^3.

As shown in Fig. 5(c) (red), the calculation is well in agreement with the experimental data at resonant and negative detuning regime ($\delta < 0$). When $\delta > 0.5$ MHz, they slightly diverge from each other, probably due to the asymmetry of the intersubband structure of QCL. Figure 5(d) shows the power dependence of $\delta f_{\text{RF-beatnote}}$. The frequency difference between the beat note and the RF is initially set to be ~0.22 MHz. Fixing the RF frequency and increasing its power, the beat note is gradually approaching toward the RF signal. Thereby, detuning $\delta f_{\text{RF-beatnote}}$ progressively decreases and finally becomes zero when falling in resonance. This experimental result is in agreement with the simulation in Fig. 3(d) (solid line). Since our device is a high-performance QCL with an output power $P_0 >$ 1 W in CW operation, the locking range is limited to ~0.35 MHz as can be directly observed in Figs. 5(a) and 5(c). However, the locking range can be further extended by increasing the RF power to satisfy the requirements of applications.

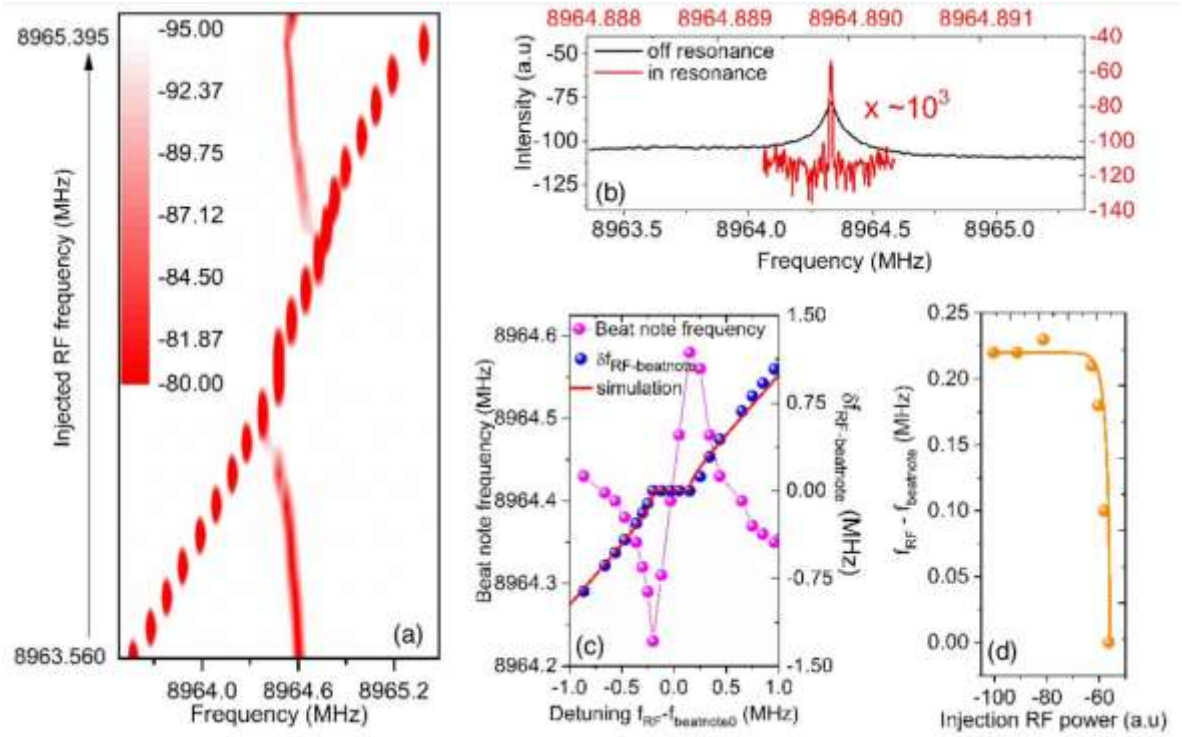

Fig. 5(a) The evolution of the beat note (continuous branch) of the QCL as a function of the injected RF frequency (discrete branch) (each injected RF frequency can be found in the x axis). (b) The beat note linewidth of the QCL at off-resonance and resonance conditions, respectively. (c) Magenta: the beat note frequency as a function of the detuning δ between RF frequency f_{RF} and the beat note without RF injection Δf_0. Blue: the frequency difference $\delta f_{RF-beatnote}$ between RF and beat note as a function of detuning δ. (d) The power dependence experiment (ball) and simulation (curve) of the frequency difference $\delta f_{RF-beatnote}$.

5. CONCLUSIONS AND PERSPECTIVES

The QCL is becoming the leading semiconductor laser source in the midinfrared frequency range thanks to the tremendous development in the past two decades. Particularly, the recent breakthroughs in high power, high efficiency QCLs, room temperature THz sources and frequency combs based on QCLs, and injection-locking high power QCLs,

are pushing QCL technology to new frontiers of research. With further development of this technology, many new QCL based applications in spectroscopy and sensing are likely to emerge in the near future.

6. ACKNOWLEDGEMENTS

This research is funded by National Science Foundation (NSF) grant number 2149908, . The support of Walter p. Murphy Chair at Northwestern / Center for Quantum Devices.

REFERENCES

1. M. Razeghi, *The MOCVD Challenge: A survey of GaInAsP-InP and GaInAsP-GaAs for photonic and electronic device applications* (CRC Press, 2010).
2. J. Faist, Quantum Cascade Lasers (OUP, Oxford, 2013).
3. Razeghi, M. A lifetime of contributions to the world of semiconductors using the Czochralski invention. J. Vacuum **146**, 308 (2017).
4. M. Razeghi, "High-Performance InP-Based Mid-IR Quantum Cascade Lasers," Ieee J Sel Top Quant **15**, 941-951 (2009).
5. M. Razeghi, W. Zhou, S. Slivken, Q. Y. Lu, D. Wu, and R. McClintock, "Recent progress of quantum cascade laser research from 3 to 12 μm at the Center for Quantum Devices [Invited]," Appl. Opt. 56(31), H30–H44 (2017).
6. M. Razeghi, Q. Y. Lu, N. Bandyopadhyay, W. Zhou, D. Heydari, Y. Bai, and S. Slivken, "Quantum cascade lasers: from tool to product," Opt Express **23**, 8462-8475 (2015).
7. N. Bandyopadhyay, Y. Bai, S. Tsao, S. Nida, S. Slivken, and M. Razeghi, "Room temperature continuous wave operation of lambda similar to 3-3.2 mu m quantum cascade lasers," Appl Phys Lett **101**, 241110 (2012).
8. Lu, Q. Y., Wu, D. H., Sengupta, S., Slivken, S., and Razeghi, M. Room temperature continuous wave, monolithic tunable THz sources based on highly efficient mid-infrared quantum cascade lasers. Sci. Reports 6, 23595 (2016).
9. Y. Bai, N. Bandyopadhyay, S. Tsao, S. Slivken, and M. Razeghi, "Room temperature quantum cascade lasers with 27% wall plug efficiency," Appl Phys Lett **98**, 181102 (2011).
10. W. J. Zhou, Q. Y. Lu, D. H. Wu, S. Slivken, M. Razeghi, High-power, continuous-wave, phase-locked quantum cascade laser arrays emitting at 8 μm. Opt Express **27**, 15776-15785 (2019).
11. A. Knigge, G. Erbert, J. Jönsson, W. Pittroff, R. Staske, B. Sumpf, M. Weyers, and G. Tränkle, "Passively cooled 940 nm laser bars with 73% wall-plug efficiency at 70 W and 25°C," Electron. Lett. 41(5), 250 (2005).
12. Y. Bai, N. Bandyopadhyay, S. Tsao, E. Selcuk, S. Slivken, and M. Razeghi, "Highly temperature insensitive quantum cascade lasers," Appl. Phys. Lett. 97(25), 251104 (2010).
13. A. Lyakh, M. Suttinger, R. Go, P. Figueiredo, and A. Todi, "5.6 μ m quantum cascade lasers based on a two-material active region composition with a room temperature wall-plug efficiency exceeding 28%," Appl. Phys. Lett. 109(12), 121109 (2016).
14. F. Wang, S. Slivken, D. H. Wu, Q. Y. Lu, and M. Razeghi, " Continuous wave quantum cascade lasers with 5.6 W output power at room temperature and 41% wall-plug efficiency in cryogenic operation," AIP Advances 10 (5), 055120 (2020).
15. F. Wang, S. Slivken, D. H. Wu, and M. Razeghi, " Room temperature quantum cascade lasers with 22% wall plug efficiency in continuous-wave operation," Opt. Express 28, 17532 (2020).
16. F. Wang, S. Slivken, D. H. Wu, and M. Razeghi, " Room temperature quantum cascade laser with … 31% wall-plug efficiency," AIP Adv. 10, 075012 (2020).

17. Q. Y. Lu, N. Bandyopadhyay, S. Slivken, Y. Bai, and M. Razeghi, "Room temperature single-mode terahertz sources based on intracavity difference-frequency generation in quantum cascade lasers," Appl Phys Lett **99**, 131106 (2011).
18. Q. Y. Lu, and M. Razeghi, " Recent advances in room temperature, high-power terahertz quantum cascade laser sources based on difference-frequency generation," Photonics **3**, 42 (2016).
19. Lu, Q. Y., Bandyopadhyay, N., Slivken, S., Bai, Y. & Razeghi, M. Widely-tuned room temperature terahertz quantum cascade laser sources based on difference frequency generation. *Appl. Phys. Lett.* **101**, 251121 (2012).
20. Lu, Q. Y., Bandyopadhyay, N., Slivken, S., Bai, Y. & Razeghi, M. High performance terahertz quantum cascade laser sources based on intracavity difference frequency generation. *Opt Express* **21**, 968 (2013).
21. Lu, Q. Y., Bandyopadhyay, N., Slivken, S., Bai, Y., and Razeghi, M., " Room temperature terahertz quantum cascade laser sources with 215 μW output power through epilayer-down mounting " Appl. Phys. Lett. **103**, 011101 (2013).
22. Lu, Q. Y., Bandyopadhyay, N., Slivken, S., Bai, Y., and Razeghi, M., "Continuous operation of a monolithic semiconductor terahertz source at room temperature," Appl. Phys. Lett. **104**, 221105 (2014).
23. Lu, Q. Y., Slivken, S., Bandyopadhyay, N., Bai, Y., and Razeghi, M. Widely tunable room temperature semiconductor terahertz source. *Appl. Phys. Lett.* **105**, 201102 (2014).
24. T. Udem, R. Holzwarth, and T. W. Hansch, "Optical frequency metrology," Nature **416**, 233-237 (2002)
25. Q. Y. Lu, M. Razeghi, S. Slivken, N. Bandyopadhyay, Y. Bai, W. J. Zhou, M. Chen, D. Heydari, A. Haddadi, R. McClintock, M. Amanti, and C. Sirtori, "High power frequency comb based on mid-infrared quantum cascade laser at lambda similar to 9 mu m," Appl Phys Lett **106**(2015).
26. Q. Y. Lu, D. H. Wu, S. Slivken, and M. Razeghi, "High efficiency quantum cascade laser frequency comb," . *Sci. Rep.* **7**, 43806 (2017).
27. Lu, Q. Y., Manna, S., Slivken, S., Wu, D. H., & Razeghi, M. Dispersion compensated mid-infrared quantum cascade laser frequency comb with high power output. *AIP Advances* **7**, 045313 (2017).
28. Lu, Q. Y., Razeghi, M., *et al*. Shortwave quantum cascade laser frequency comb for multi-heterodyne spectroscopy. *Appl. Phys. Lett.* **112**, 141104 (2018).
29. Lu, Q. Y., Wang, F. H., Wu, D. H., Slivken, S., & Razeghi, M. Room temperature terahertz semiconductor frequency comb, *Nature Commun.* **10**, 2403 (2019).
30. C. D. Nabors, A. D. Farinas, T. Day, S. T. Yang, E. K. Gustafson, and R. L. Byer, "Injection locking of a 13-W cw Nd:YAG ring laser," Opt. Lett. 14, 1189–1191 (1989).
31. F. R. Ahmad and F. Rana, "Fundamental and subharmonic hybrid mode-locking of a high-power (220 mW) monolithic semiconductor laser," IEEE Photon. Technol. Lett. 20, 1308–1310 (2008).
32. U. Keller, "Recent developments in compact ultrafast lasers," Nature 424, 831–838 (2003).
33. G. E. Villanueva, M. Ferri, and P. Perez-Millan, "Active and passive mode-locked fiber lasers for highspeed high-resolution photonic analog-to-digital conversion," IEEE J. Quantum Electron. 48, 1443–1452 (2012).
34. F. F. Voigt, F. Emaury, P. Bethge, D. Waldburger, S. M. Link, S. Carta, A. van der Bourg, F. Helmchen, and U. Keller, "Multiphoton in vivo imaging with a femtosecond semiconductor disk laser," Biomed. Opt. Express 8, 3213–3231 (2017).
35. J. J. McFerran, "Échelle spectrograph calibration with a frequency comb based on a harmonically modelocked fiber laser: a proposal," Appl. Opt. 48, 2752–2759 (2009).
36. F. Wang, V. Pistore, M. Riesch, H. Nong, P.-B. Vigneron, R. Colombelli, O. Parillaud, J. Mangeney, J. Tignon, C. Jirauschek, and S. S. Dhillon, "Ultrafast response of harmonic modelocked THz lasers," Light Sci. Appl. 9, 51 (2020).
37. D. G. Revin, M. Hemingway, Y. Wang, J. W. Cockburn, and A. Belyanin, "Active mode locking of quantum cascade lasers in an external ring cavity," Nat. Commun. 7, 11440 (2016).

38. J. Hillbrand, N. Opačak, M. Piccardo, H. Schneider, G. Strasser, F. Capasso, and B. Schwarz, “Modelocked short pulses from an 8 μm wavelength semiconductor laser,” Nat. Commun. 11, 5788 (2020).
39. F. Wang, S. Slivken, and M. Razeghi, "Harmonic injection locking of high-power mid-infrared quantum cascade lasers," Photonics Research 9 (6), 1078-1083 (2021).